Hindawi
Journal of Nanomaterials
Volume 2022, Article ID 2738398, 9 pages
https://doi.org/10.1155/2022/2738398

Research Article

Analysis of Natural Convection in Nanofluid Flow through a Channel with Source/Sink Effect

Imran Siddique,[1] **Kashif Sadiq**,[1] **Fahd Jarad**,[2,3,4] **Mohammed K. Al Mesfer**,[5] **Mohd Danish**,[5] **and Sonia Yaqoob**[1]

[1]*Department of Mathematics, University of Management and Technology, Lahore 54770, Pakistan*
[2]*Department of Mathematics, Cankaya University, 06790, Etimesgut, Ankara, Turkey*
[3]*Department of Mathematics, King Abdulaziz University, Jeddah, Saudi Arabia*
[4]*Department of Medical Research, China Medical University Hospital, China Medical University, Taichung, Taiwan*
[5]*Chemical Engineering Department, College of Engineering, King Khalid University, Abha, Saudi Arabia*

Correspondence should be addressed to Fahd Jarad; fahd@cankaya.edu.tr

Received 9 November 2021; Revised 22 February 2022; Accepted 6 April 2022; Published 4 May 2022

Academic Editor: Taza Gul

In this study, the natural convection nanofluids flow through a channel formed by two vertical parallel plates having distance d between them has been examined under the influence of the ramped velocity. Sodium alginate is considered as base fluid, and nanoparticles of titania (TiO_2) and alumina (Al_2O_3) are added to it. Analytical and semianalytical results for temperature and velocity profiles are obtained with Laplace transform and inverse Laplace algorithms (Tzou, Stehfest, Talbot, Honig and Hirdes, and Fourier series), respectively. Furthermore, the impacts of nanoparticles, Prendtl number, heat absorption, and time on velocity and temperature are drawn graphically and discussed. The outcomes show that the high thermal conductivity of particles increases the temperatures, and the high density of particles decreases the velocities of the nanofluids. The current findings are compared to previous findings in the literature. In the tables, the effect of volume fraction on Nusselt numbers and skin frictions is explored.

1. Introduction

The study of viscous fluid between parallel plates is significant due to its vast applications in the science and engineering fields. Sahebi et al. [1] presented the analysis of the free convection non-Newtonian nanofluid flow in a vertical channel numerically and described its significance. Many engineers studied the flow of non-Newtonian fluids with constant physical properties and heat transport, manipulating problems related to fluid mechanics and heat transfer. Adesanya [2] studied the unsteady free convection flow with absorbing generation between two infinite parallel plates with a temperature jump and velocity slip in the slip flow regime. Boulama and Galanis [3] provided the exact results for mixed convection nanofluid flow between two plates with mass and heat transfer. Ajibade and Bichi [4] studied an unsteady incompressible convective fluid flow that is optically dense through an upright channel due to the collective effect of thermal radiation and variable viscosity and concluded that by increasing the viscosity variation parameters and thermal radiation, the velocity of fluid increases and temperature also increases with a boost in thermal radiation. Rajkumar et al. [5] investigated the numerical results of the inner convection of heat sources in tandem planar. Nada [6] studied the heat transport rate of free convection flow in horizontally and vertically closed narrow heated finned base plates, and the outcomes confirmed that the fins increase the rate of heat exchange with fin array geometries. Usually, the concentration disparity in the mass transfer influences the rate of heat relocation. The buoyancy effects are the driving forces for natural convection.

Several researchers discussed their work on nanofluids. The idea of nanofluid was given by Eastman and Choi [7]. Nanofluid allocates the fluid in which the nanoparticles are hanging in the traditional fluid. Because of the rapid advancement of nanotechnology [8], various models of nanofluids are being implemented in the field of thermal engineering. So nanofluid shows more effective thermal conductivity as compared with the base fluid. Suspended components raise thermal conduction and heat conveyance processes as the solid bimetallic particles bear more caloric conductivity than the base fluid. High viscosity and more static with better diffusion, wetting, and propagation through solid aerofoils, even for minor nanoparticle addition, are significant features of nanofluids [9]. Nanofluids are comprised of super-fine nanoparticles (size < 100 nm) mixed in water or organic solvent [10].

Generally, nanoparticles of chemically stable materials like copper (Cu), gold (Au), silicon oxide (SiO_2) or silica, zirconium oxide (ZrO_2), titania (TiO_2), copper oxide (CuO), alumina (Al_2O_3), metallic nitrides (SiN, AlN), and carbon nanotubes (CNTs) are used. These solid-liquid specks quickly drop down, filled the flow ducts, serious pressure failure, and causing erosion of pipelines. Therefore because of these defects, ordinary solid-fluid fusions for heat change at micro levels are used instead of nanofluids. Nanofluids can increase critical temperatures and surfactants, or standard emulsifiers cannot increase thermal conductivity. Cooling plays important role in providing comfort for required functioning and well-founded results of developing products especially computers, electronic circuits, X-ray generators, automobile engines, high energy lasers, etc. Improvement of heat transferal characteristics of nanofluids stimulates the attainable development in the heating system or consignment and heat flows caused by power in small-scaled products elevated its applications in defensive structure, microelectronics, fabricating, transportation, metrology, and engine cooling system.

The researchers have conducted extensive studies in this field. Some investigations are experimental, while others are computational, and only a small amount of research has been undertaken on the analytical side. The efficacy of carbon nanostructures and water-based nanoliquids as coolants was investigated by Halelfadl et al. [11]. They looked at how low nanoparticle volume fractions (varying from 0.0055% to 0.278%) affected nanofluid density, thermal conductivity, and viscosity.

Solar thermal devices' efficiency and performance could be improved. The use of nanotechnology in solar collectors has been the subject of extensive research. Solar cells are heat engines that capture sunlight and transmit the heat to a liquid running past them. Tyagi et al. [12] discovered that adding nanoparticles to a collector improves its efficiency. His findings reveal that by changing the volume fraction from 0.1% to 2% and the size of the fraction, the efficiency increases dramatically. When compared to water, Yousefi et al. [13] discovered that nanofluid (with 0.2% wt.) had a higher efficiency. When they added surfactant to their trials, they saw a 15.63% improvement [14, 15], and the references therein include examples of nanoparticles in solar energy applications.

Fluid flow and linked mass and energy transmission through a channel have received less attention than the situation of a single plate. This design may be found in a wide range of fields, such as petroleum reservoirs, fire engineering, combustion modeling, and nuclear energy, to name a few. Many engineering systems show transport phenomena that combine the effects of concentration and thermal buoyancy. Modern thermal protection devices, chemical distilleries, building ventilation systems, solar panels, heat exchangers, and electric circuits all contain them [16, 17]. Gupta et al. [18] used Marangoni convection to study the flow of two separate nanofluids over a stretched surface in a porous medium. Gohar et al. [19] investigated a Darcy-Forchheimer flow of Casson hybrid nanofluid via a curved surface that was constantly growing. The viscous fluid flow in a porous medium is expressed by the Darcy-Forchheimer effect. Adnan et al. [20] investigated the flow of Cu-water and Cu-kerosene oil through two Riga plates, taking into account surface convection and radiation effects. Zaka Ullah et al. [21] studied the flow of a hybrid nanofluid in a diverging and a converging channel. The effects of ramped temperature, ramped concentration, chemical reaction, heat production, and magnetic force on Casson nanofluid flow via a conduit were studied by Sadiq et al. [22]. The influence of various fluid dynamical processes and flow geometry is the focus of the bulk of the study. In addition, the bulk of previous research was conducted using either experimental or numerical methods.

The energy storage devices are beneficial for regulating power and energy demand in concentrated solar power facilities. It is expected that increasing the capacity of materials used in total energy storage will increase their performance. As a result, the leading objective of this dissertation is to establish a solution to the problem of natural convection flow of two different nanofluids in a vertical channel under the influence of ramped velocity. Ramped wall velocity is useful to control the flow of the fluid. To the best of the author's knowledge, ramped velocity is not considered for this model. Sodium alginate (SA) is taken as a base fluid having nanoparticles of titania (TiO_2) and alumina (Al_2O_3) is studied. Analytical and semianalytical results for velocity field and temperature distribution are obtained by using the Laplace transform method and inverse numerical algorithms (Stehfest's [23], Tzou's [24], Talbot [25], Honig and Hirdes [26], and Fourier series [27]). Finally, the effects of nanoparticles, Prandtl number, heat absorption, and time on temperature and velocity profiles are graphically illustrated and discussed. The current findings are compared to previous findings in the literature. In the tables, the effect of volume fraction on Nusselt numbers and skin frictions is explored. The findings of this study are predicted to have a significant impact on solar thermal devices.

2. Mathematical Formulation

Consider the convective flow of two different nanofluids with ramped velocity in a vertical channel formed by two parallel infinite plates separated by a distance d in the presence of the source/sink effect. The left plate is considered

along the x'-axis as shown in Figure 1. At $t' = 0$, the nanofluid and plates are at rest at a moderate temperature T_0. At $t' > 0$, the right plate which is situated at $y' = d$ begins to accelerate along x'-direction with $A_0 t'$, and temperatures of left and right plate are remained constant T_1 and T_2 ($T_2 > T_1$), respectively. The slippage between nanoparticles and base fluid is neglected.

The heat and momentum are only the functions of y' and t' as the walls of the channel are extended infinitely. Sodium alginate (SA) is considered as a conventional base fluid having nanoparticles of titania (TiO_2) and alumina (Al_2O_3). The thermophysical characteristics of SA and nanoparticles are given in Table 1.

Under the above assumptions, the governing equations are [30]

$$\rho_{nf}\frac{\partial u'\left(y',t'\right)}{\partial t'} = \mu_{nf}\frac{\partial^2 u'\left(y',t'\right)}{\partial y'^2} + g(\rho\beta)_{nf}\left[T'\left(y',t'\right) - T_1\right], \tag{1}$$

$$\left(\rho c_p\right)_{nf}\frac{\partial T'\left(y',t'\right)}{\partial t'} = k_{nf}\frac{\partial^2 T'\left(y',t'\right)}{\partial y'^2} - Q_0\left[T'\left(y',t'\right) - T_1\right], \tag{2}$$

with corresponding conditions

$$u'\left(y',0\right) = 0, T'\left(y',0\right) = T_1, 0 \le y' \le d, \tag{3}$$

$$u'\left(0,t'\right) = 0, u'\left(d,t'\right) = A_0 t', t' > 0, \tag{4}$$

$$T'\left(0,t'\right) = T_1, T'\left(d,t'\right) = T_2, t' > 0. \tag{5}$$

The thermal physical features of nanofluid are described by

$$\rho_{nf} = \varphi\rho_s + (1-\varphi)\rho_f, \mu_{nf}(1-\varphi)^{2.5} = \mu_f,$$
$$k_{nf} = \frac{\left(k_f - k_s\right)\varphi + 2k_f + k_s}{k_s - 2\left(k_f - k_s\right)\varphi + 2k_f}k_f,$$
$$\frac{(\rho\beta)_{nf}}{(\rho\beta)_f} = (1-\varphi) + \varphi\frac{(\rho\beta)_s}{(\rho\beta)_f}, \frac{\left(\rho c_p\right)_{nf}}{\left(\rho c_p\right)_f} = (1-\varphi) + \varphi\frac{\left(\rho c_p\right)_s}{\left(\rho c_p\right)_f}. \tag{6}$$

Introducing the following non-dimensional parameters into Eqs. (1)–(5).

$$u = \frac{u'\nu_f}{A_0 d^2}, y = \frac{y'}{d}, t = \frac{\nu_f}{d^2}t', T = \frac{T' - T_1}{T_2 - T_1}, \tag{7}$$

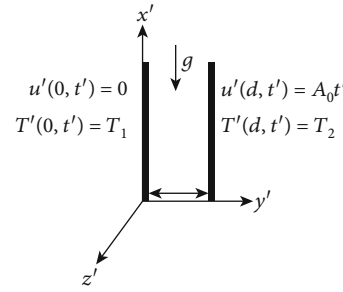

Figure 1: Flow geometry.

we get

$$\frac{\partial u(y,t)}{\partial t} = p_1\frac{\partial^2 u(y,t)}{\partial y^2} + p_2 T(y,t), \tag{8}$$

$$\frac{\partial T(y,t)}{\partial t} = p_3\frac{\partial^2 T(y,t)}{\partial y^2} - p_4 T(y,t), \tag{9}$$

with corresponding conditions,

$$T(y,0) = 0, u(y,0) = 0; 0 \le y \le 1, \tag{10}$$

$$T(0,t) = 0, u(0,t) = 0; t > 0, \tag{11}$$

$$T(1,t) = 1, u(1,t) = t; t > 0, \tag{12}$$

where

$$p_1 = \frac{\mu_{nf}}{\rho_{nf}\nu_f}, p_2 = Gr\frac{\beta_{nf}}{\beta_f}, p_3 = \frac{1}{Pr}\frac{k_{nf}}{k_f}\frac{\left(\rho c_p\right)_f}{\left(\rho c_p\right)_{nf}}, p_4 = Q\frac{\left(\rho c_p\right)_f}{\left(\rho c_p\right)_{nf}},$$
$$Gr = \frac{g(\beta)_f(T_2 - T_1)}{A_0}, Pr = \frac{\nu_f\left(\rho c_p\right)_f}{k_f}, Q = \frac{Q_0 d^2}{\nu_f\left(\rho c_p\right)_f}. \tag{13}$$

3. Solution of the Problem

3.1. Temperature Profile. Applying the Laplaceitransformito Eqs. (9), $(11)_1$, and $(12)_1$, using Eq. $(10)_1$, we obtain

$$s\bar{T}(y,s) = p_3\frac{\partial^2\bar{T}(y,s)}{\partial y^2} - p_4\bar{T}(y,s), \tag{14}$$

$$T(0,s) = 0, \bar{T}(1,s) = \frac{1}{s}. \tag{15}$$

Solution of Eq. (14) with the conditions in Eq. (15) is as

$$\bar{T}(y,s) = \frac{\sinh\sqrt{s + p_4/p_3}y}{s.\sinh\sqrt{s + p_4/p_3}}, \tag{16}$$

Table 1: Thermophysical characteristics of nanoparticles and SA [28, 29].

Material	k(W/m.K)	$\beta \times 10^5\ (K^{-1})$	C_p(J/Kg.K)	ρ(Kg/m^3)
Sodium alginate $C_6H_9NaO_7$ (SA)	0.6376	0.99	4175	989
Titania (TiO_2)	8.9538	0.90	686.2	4250
Alumina (Al_2O_3)	40	0.85	765	3970

Table 2: Variation of Nusselt numbers.

φ	t	TiO_2		Al_2O_3	
		$y = 0$	$y = 1$	$y = 0$	$y = 1$
0	0.5	-0.118	-2.989	-0.118	-2.989
0.01	0.5	-0.129	-3.024	-0.131	-3.031
0.05	0.5	-0.185	-3.164	-0.197	-3.198
0.10	0.5	-0.273	-3.344	-0.305	-3.413

or

$$\bar{T}(y,s) = \sum_{n=0}^{\infty}\left[\frac{1}{s}\exp\left[-\left(\frac{(2n+1)}{\sqrt{p_3}} - \frac{y}{\sqrt{p_3}}\right)\sqrt{s+p_4}\right] - \frac{1}{s}\exp\left[-\left(\frac{(2n+1)}{\sqrt{p_3}} + \frac{y}{\sqrt{p_3}}\right)\sqrt{s+p_4}\right]\right]. \tag{17}$$

The inverse Laplace transform of Eq. (17) is

$$\begin{aligned} T(y,t) = {} & \frac{1}{2}\sum_{n=0}^{\infty}\exp\left(\frac{\sqrt{p_4}}{\sqrt{p_3}}(2n+1-y)\right) \cdot \left[\operatorname{erfc}\left(\frac{2n+1-y}{2\sqrt{p_3 t}} + \sqrt{p_4 t}\right) + e\operatorname{rfc}\left(\frac{2n+1-y}{2\sqrt{p_3 t}} + \sqrt{p_4 t}\right)\right] \\ & - \frac{1}{2}\sum_{n=0}^{\infty}\exp\left(\frac{\sqrt{p_4}}{\sqrt{p_3}}(2n+1+y)\right) \cdot \left[\operatorname{erfc}\left(\frac{2n+1+y}{2\sqrt{p_3 t}} + \sqrt{p_4 t}\right) + \operatorname{erfc}\left(\frac{2n+1+y}{2\sqrt{p_3 t}} + \sqrt{p_4 t}\right)\right]. \end{aligned} \tag{18}$$

3.2. Velocity Field. Applying the Laplace transform to Eqs. (8), $(11)_2$, and $(12)_2$, using Eq. $(10)_2$, we obtain

$$s\bar{u}(y,s) = p_1\frac{\partial^2\bar{u}(y,s)}{\partial y^2} + p_2\bar{T}(y,s). \tag{19}$$

$$\bar{u}(0,s) = 0,\ \bar{u}(1,s) = \frac{1}{s^2}. \tag{20}$$

Putting the value of $\bar{T}(y,s)$ from Eq. (16) in Eq. (19), we have

$$s\bar{u}(y,s) = p_1\frac{\partial^2\bar{u}(y,s)}{\partial y^2} + p_2\frac{\sinh\sqrt{s+p_4/p_3}y}{s.\sinh\sqrt{s+p_4/p_3}}. \tag{21}$$

Solution of Eq. (21) with the conditions in Eq. (20) is as

$$\bar{u}(y,s) = \frac{p_2p_3s + p_1p_4 - (p_3-p_1)s}{(p_1p_4-(p_3-p_1)s)s^2}\frac{\sinh\left(y\left(\sqrt{s}/\sqrt{p_1}\right)\right)}{\sinh\left(\sqrt{s}/\sqrt{p_1}\right)} - \frac{p_2p_3}{(p_1p_4-(p_3-p_1)s)s}\frac{\sinh\left(y\left(\sqrt{s+p_4}/\sqrt{p_3}\right)\right)}{\sinh\left(\sqrt{s+p_4}/\sqrt{p_3}\right)}, \tag{22}$$

or

$$\bar{u}(y,s) = \frac{1}{s}\frac{\sinh\left(\left(y/\sqrt{p_1}\right)\sqrt{s}\right)}{s.\sinh\left(\sqrt{s}/\sqrt{p_1}\right)} - \frac{a_1}{s-a_2}\frac{\sinh\left(\left(y/\sqrt{p_1}\right)\sqrt{s}\right)}{s.\sinh\left(\sqrt{s}/\sqrt{p_1}\right)} + \frac{a_1}{s-a_2}\frac{\sinh\left(\left(\sqrt{s+p_4}/\sqrt{p_3}\right)y\right)}{s.\sinh\left(\sqrt{s+p_4}/\sqrt{p_3}\right)}, \tag{23}$$

where $a_1 = p_2p_3/p_3 - p_1, a_2 = p_1p_4/p_3 - p_1$.

The inverse Laplace transform of Eq. (23) is

$$\begin{aligned} u(y,t) = {} & \left(1 - a_1e^{a_2t}\right) * \sum_{n=0}^{\infty}\left[\psi_n\left(\frac{y}{\sqrt{p_1}}, t, 0, \frac{1}{\sqrt{p_1}}\right) - \psi_n\left(-\frac{y}{\sqrt{p_1}}, t, 0, \frac{1}{\sqrt{p_1}}\right)\right] + \left(a_1e^{a_2t}\right) \\ & * \sum_{n=0}^{\infty}\left[\psi_n\left(\frac{y}{\sqrt{p_3}}, t, p_4, \frac{1}{\sqrt{p_3}}\right) - \psi_n\left(-\frac{y}{\sqrt{p_3}}, t, p_4, \frac{1}{\sqrt{p_3}}\right)\right], \end{aligned} \tag{24}$$

where

$$\psi_n(x,\tau,y,z) = \frac{1}{2}\left[e^{-[(2n+1)z-x]\sqrt{y}}\operatorname{erfc}\left(\frac{(2n+1)z-x}{2\sqrt{\tau}} - \sqrt{y\tau}\right) + e^{[(2n+1)z-x]\sqrt{y}}\operatorname{erfc}\left(\frac{(2n+1)z-x}{2\sqrt{\tau}} + \sqrt{y\tau}\right)\right]. \tag{25}$$

Table 3: Variation of skin frictions.

φ	t	TiO_2		Al_2O_3	
		$y = 0$	$y = 1$	$y = 0$	$y = 1$
0	0.5	-0.52	-0.085	-0.52	-0.085
0.01	0.5	-0.53	-0.108	-0.532	-0.106
0.05	0.5	-0.576	-0.207	-0.583	-0.197
0.10	0.5	-0.647	-0.344	-0.659	-0.327

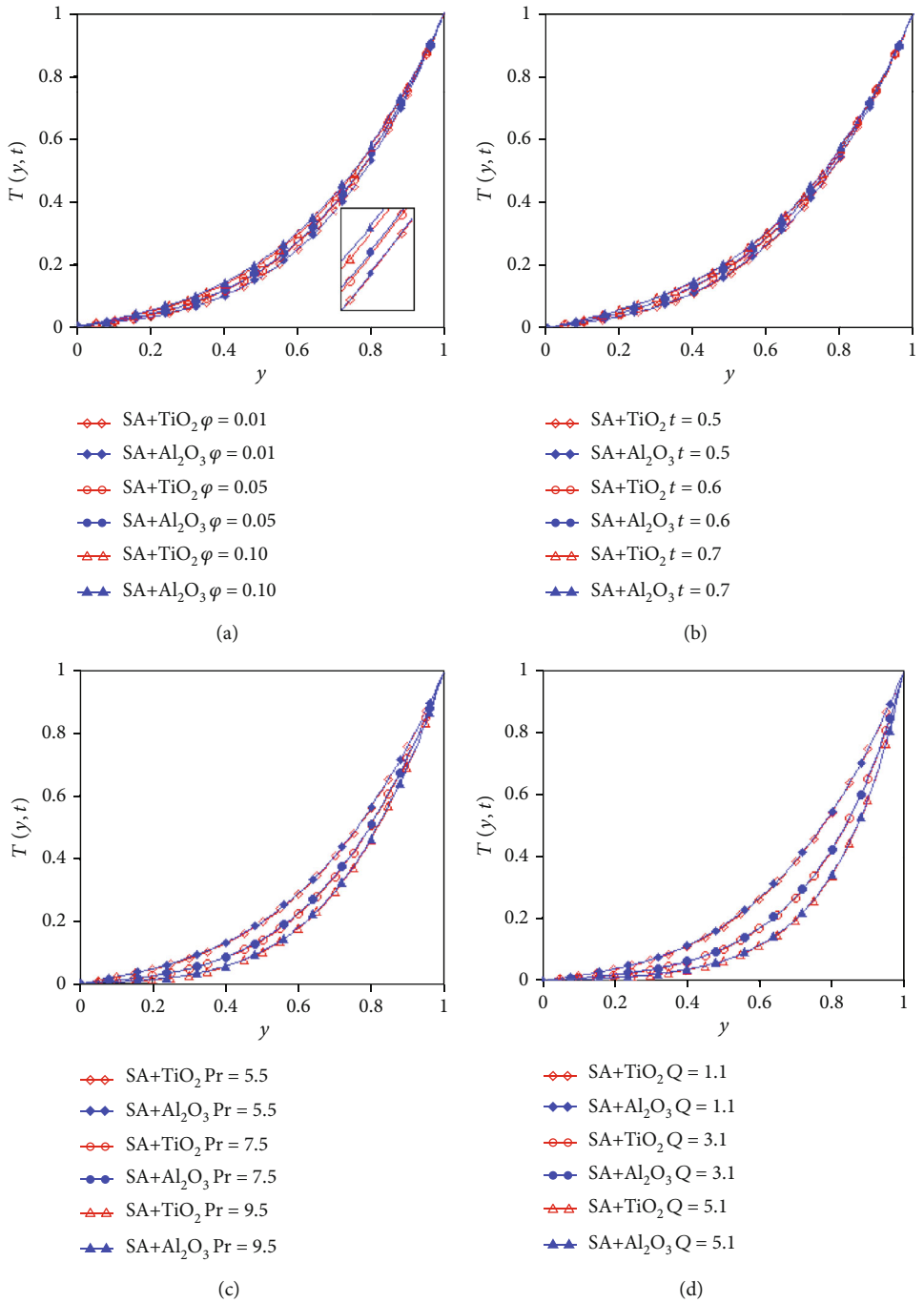

Figure 2: Variation of temperature fields.

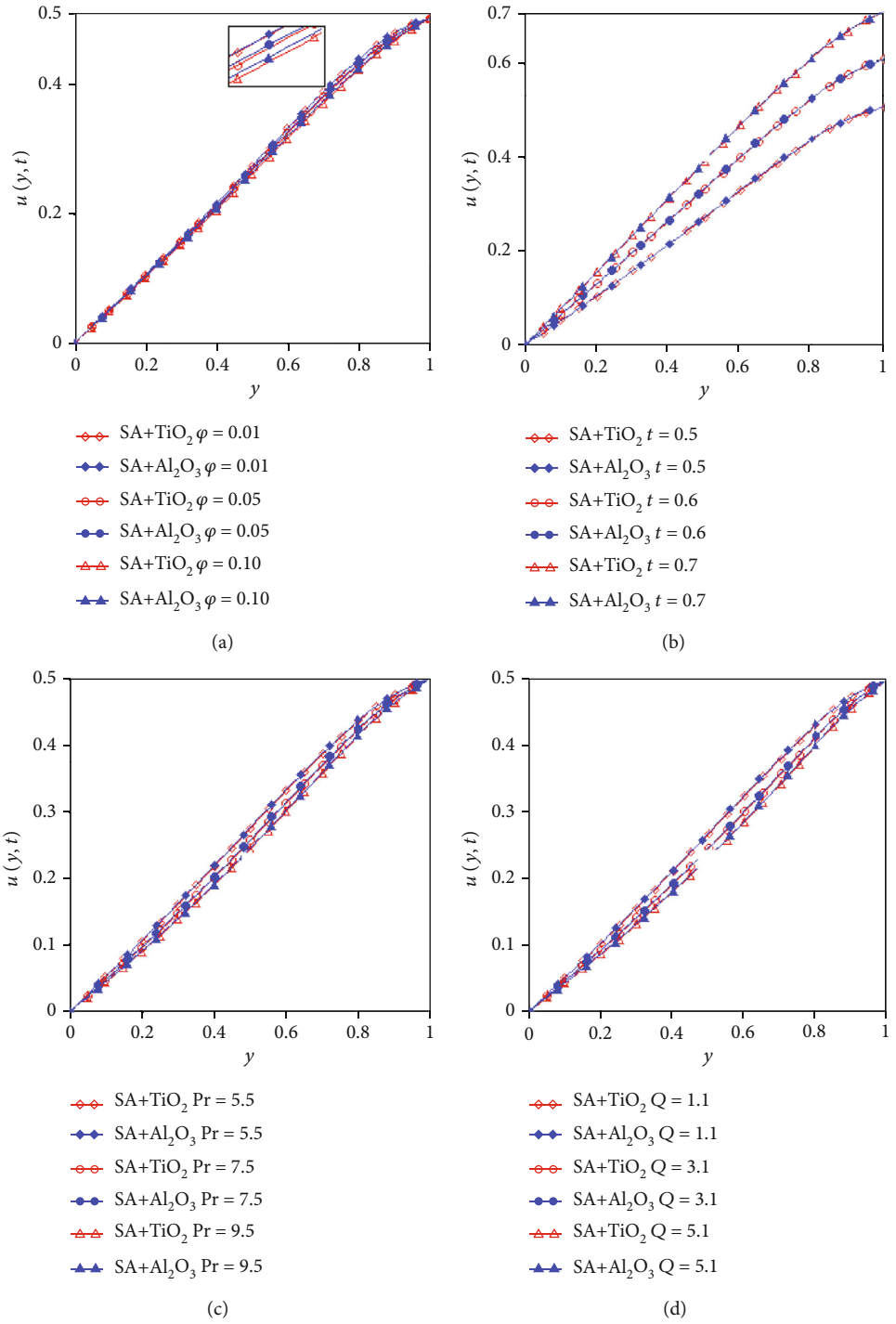

Figure 3: Variation of the velocity fields.

4. Nusselt Numbers and Skin Frictions

The Nusselt numbers and skin frictions on both walls of the channel can express as

$$\text{Nusseltnumbers} = Nu_{0,1} = -\frac{k_{nf}}{k_f} L^{-1}\left\{\frac{\partial \overline{\theta}(y,s)}{\partial y}\right\}_{y=0,1}, \tag{26}$$

$$\text{skinfrictions} = Sk_{0,1} = -\frac{\mu_{nf}}{\mu_f} L^{-1}\left\{\frac{\partial \overline{u}(y,s)}{\partial y}\right\}_{y=0,1}.$$

5. Numerical Results and Discussions

The flow of two different SA-based nanofluids with natural convection and ramped velocity is compared in this section. The influence of volume fraction and time on flow and

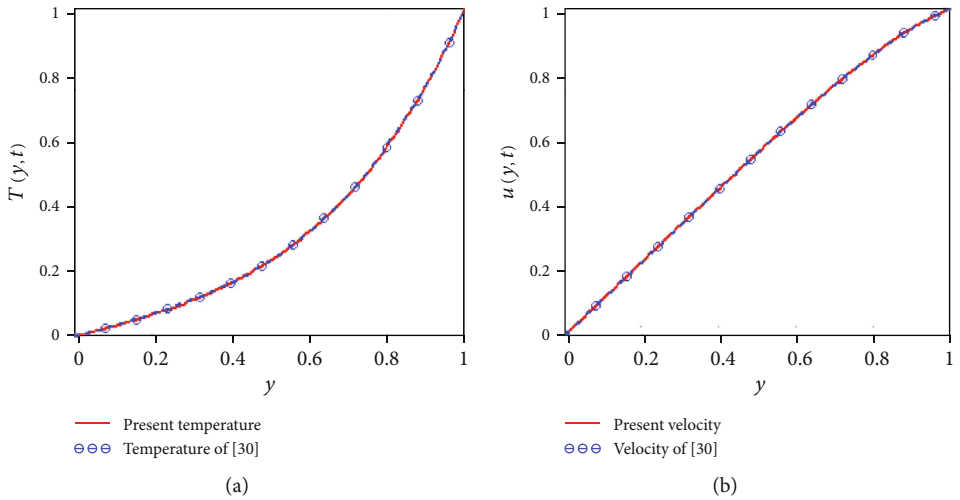

Figure 4: Comparison of results.

Table 4: Comparison of temperature profile with different Laplace inversion algorithms.

y	Results Eq. (18)	Stehfest's	Tzou's	Honing and Hirdes	Fourier series	Talbot
0	0	0	0	0	0	0
0.1	3×10^{-10}	5.2×10^{-8}	2.4×10^{-6}	1.1×10^{-8}	3×10^{-9}	3×10^{-10}
0.2	1.1×10^{-7}	3.3×10^{-7}	6×10^{-6}	1.59×10^{-7}	1.3×10^{-7}	1×10^{-7}
0.3	4.1×10^{-6}	4.6×10^{-6}	1.8×10^{-5}	4.06×10^{-6}	4×10^{-6}	4×10^{-6}
0.4	7.7×10^{-5}	9×10^{-5}	1.1×10^{-4}	7.75×10^{-5}	7.7×10^{-5}	7×10^{-5}
0.5	9.9×10^{-4}	9×10^{-4}	1×10^{-3}	9.1×10^{-4}	9.8×10^{-4}	9×10^{-4}
0.6	9×10^{-3}	8.4×10^{-3}	8.5×10^{-3}	8.41×10^{-3}	8.4×10^{-3}	9×10^{-3}
0.7	0.048	0.048	0.048	0.048	0.048	0.048
0.8	0.188	0.188	0.188	0.188	0.188	0.188
0.9	0.51	0.51	0.51	0.51	0.51	0.51
1	1	1.001	1.003	0.949	1	1

temperature is highlighted graphically and discussed. Furthermore, the results of this problem are compared by using different numerical inversion algorithms in Tables 2–3. In the graphical comparison, all parameters $Q = 1.1$, $Pr = 6.2$, $\varphi = 0.04$, $t = 0.5$, and $Gr = 3.8$ are fixed.

Figure 2(a) illustrates the variation and comparison of temperature profiles of two different nanofluids. The temperatures increase by increasing φ. The inclusion of nanoparticles increases the heat transport rate of nanofluids. Figure 2(b) depicts that the temperatures of nanofluids rise as time rises. The temperature of nanofluid-containing particles of Al_2O_3 is higher due to greater thermal conductivity. Figures 2(c) and 2(d) show the influence of Prandtl number and heat absorption on temperatures. The temperature fields of the nanofluids are shown to be lower when Pr and Q are increased.

Figure 3(a) indicates that the thickness of nanofluids increases with an increase of φ due to the higher density of nanoparticles as a result velocities reduce. The velocity of SA + TiO_2 is higher than SA + Al_2O_3 due to the low density of TiO_2. Figure 3(b) illustrates that the velocities of both fluids increase with increasing time. The influence of Prandtl number and heat absorption on the velocity profiles is seen in Figures 3(c) and 3(d). The velocities of nanofluids decrease with an increase in Pr and Q.

The authenticity of our results obtained for temperature and velocity is presented in Figure 4 by comparing them to the results of Hajizadeh et al. [30]. These figures show that for $t = 1$, our outcomes are equivalent to those found in [30]. The coinciding curves demonstrate the veracity of our findings.

Table 2 shows that when the volume fraction of nanoparticles rises, the heat transfer rate decreases on both plates. Table 3 displays the quantitative data of skin friction, which is decreased when the volume fraction values on both plates rise for two nanofluids.

Tables 4 and 5 show the comparison of our analytical solutions (18) and (24), with the semianalytical solutions obtained by different numerical inverse Laplace transform algorithms (Stehfest's [23], Tzou's [24], Fourier series [25], Talbot [26], and Honig and Hirdes [27]). From these figures and tables, it can be seen that all the numerical inverse

Table 5: Comparison of velocity profile with different Laplace inversion algorithms.

y	Results Eq. (24)	Stehfest's	Tzou's	Honing and Hirdes	Fourier series	Talbot
0	0	0	0	0	0	0
0.1	0.964	0.964	0.965	0.976	0.967	0.964
0.2	1.93	1.93	1.93	1.954	1.934	1.93
0.3	2.898	2.898	2.899	2.934	2.904	2.898
0.4	3.869	3.869	3.87	3.918	3.878	3.869
0.5	4.845	4.845	4.847	4.906	4.856	4.845
0.6	5.827	5.827	5.829	5.9	5.84	5.827
0.7	6.816	6.816	6.819	6.901	6.831	6.816
0.8	7.81	7.81	7.812	7.906	7.826	7.81
0.9	8.758	8.758	8.76	8.866	8.776	8.758
1	9.379	9.379	9.381	9.497	9.399	9.379

Laplace transform algorithms have good agreement with our obtained results.

6. Conclusion

The focus of this work is to examine the results of the convective flow of two nanofluids in an upright channel with ramped velocity. Analytical results of temperature and velocity fields are attained by using the Laplace transform technique. Sodium alginate is considered a base fluid, and nanoparticles of TiO_2 and Al_2O_3 are added to it. Analytical and semianalytical results are compared. The effects of time, Prandtl number, heat absorption, and volume fraction are discussed in detail. The current findings are compared to previous findings in the literature. In the tables, the effect of volume fraction on Nusselt numbers and skin frictions is explored. The main observations are as follows:

(i) The temperature profiles increase for higher values of φ due to greater thermal conductivities

(ii) The velocity fields decrease for greater values of φ due to high densities

(iii) The velocity and temperature fields are increasing function of time t

(iv) The nanoparticles (Al_2O_3) increase temperature much more than the nanoparticles (TiO_2)

(v) The velocity is less when the nanoparticles alumina (Al_2O_3) is added in base fluid than by adding the nanoparticles titania (TiO_2)

(vi) The velocity can be controlled and predicted with ramped velocity conditions

(vii) The thickness of nanofluids increases due to higher viscosity caused by greater values of Pr in return velocity and temperature reduces

(viii) The momentum and energy of nanofluids are reduced for higher values of Q

(ix) Nusselt numbers and skin frictions decrease on both walls of channel for both nanofluids by increasing φ

(x) The solutions obtained by different methods are in good agreement

Nomenclature

u': Velocity
T': Temperature
g: Gravitational acceleration
ρ_{nf}: Density
Gr: Grashof number
β_{nf}: Thermal expansion
μ_{nf}: Dynamic viscosity
Q_0: Source/sink effect
$(c_p)_{nf}$: Specific heat
Pr: Prandtl number
d: Distance between plates
Q: Dimensionless source/sink effect
φ: Volume fraction
Sk: Skin friction
Nu: Nusselt number
s: Solid particles
nf: Nanofluid
f: Fluid.

Data Availability

The data used to support the findings of this study are available from the corresponding author upon request.

Conflicts of Interest

The authors declare that they have no conflicts of interest.

Acknowledgments

This study was funded by Deanship of Scientific Research (Project no. RGP. 1/161/42), King Khalid University, Abha, Saudi Arabia.

References

[1] S. A. R. Sahebi, H. Pourziaei, A. R. Feizi, M. H. Taheri, Y. Rostamiyan, and D. D. Ganji, "Numerical analysis of natural convection for non-Newtonian fluid conveing nanoparticles between two vertical parallel plates," *The European Physical Journal*, vol. 1, no. 2, pp. 130–238, 2015.

[2] S. O. Adesanya, "Free convective flow of heat generating fluid through a porous vertical channel with velocity slip and temperature jump," *Engineering Physics and Mathematics*, vol. 6, no. 3, pp. 1045–1052, 2015.

[3] K. Boulama and N. Galanis, "Analytical solution for fully developed mixed convection between parallel vertical plates with heat and mass transfer," *ASME journal of heat transfer*, vol. 126, no. 3, pp. 381–388, 2004.

[4] A. O. Ajibade and Y. A. Bichi, "Unsteady natural convection flow through a vertical channel due to the combined effects of variable viscosity and thermal radiation," *Journal of Applied and Computational Mathematics*, vol. 7, no. 3, p. 403, 2018.

[5] M. R. Rajkumar, G. Venugopal, and S. A. Lal, "Natural convection from free standing tandem planar heat sources in a vertical channel," *Applied Thermal Engineering*, vol. 50, no. 1, pp. 1386–1395, 2013.

[6] S. A. Nada, "Natural convection heat transfer in horizontal and vertical closed narrow enclosures with heated rectangular finned base plate," *International Journal of Heat and Mass Transfer*, vol. 50, no. 3-4, pp. 667–679, 2007.

[7] S. U. S. Choi and J. A. Eastman, *Enhancing Thermal Conductivity of Fluids with Nanoparticles*, ASME IMECC, ASMEI-MECC, San Francisco, USA, 1995.

[8] Y. Xuan and Q. Li, "Investigation on convective heat transfer and flow features of nanofluids," *Journal of Heat Transfer*, vol. 125, no. 1, pp. 151–155, 2003.

[9] S. Shateyi and J. Prakash, "A New Numerical Approach for MHD Laminar Boundary Layer Flow and Heat Transfer of Nanofluids over a Moving Surface in the Presence of Thermal Radiation," *Boundary value problems*, vol. 2014, no. 1, 2014.

[10] S. U. S. Choi, "Nanofluids from vision to reality through research," *Journal of Heat Transfer*, vol. 131, pp. 1–9, 2009.

[11] S. Halelfadl, T. Maré, and P. Estellé, "Efficiency of carbon nanotubes water based nanofluids as coolants," *Experimental Thermal and Fluid Science*, vol. 53, pp. 104–110, 2014.

[12] H. Tyagi, P. Patrick, and R. Prasher, "Predicted efficiency of a low temperature nanofluidbased direct absorption solar collector," *Journal of Solar Energy Engineering*, vol. 131, no. 4, 2009.

[13] T. Yousefi, F. Veysi, E. Shojaeizadeh, and S. Zinadini, "An experimental investigation on the effect of Al_2O_3-H_2O nanofluid on the efficiency of flat-plate solar collectors," *Renewable Energy*, vol. 39, no. 1, pp. 293–298, 2012.

[14] H. Zamani, O. Mahian, I. Rashidi, G. Lorenzini, and S. Wongwises, "Exergy optimization of a double-exposure solar cooker by response surface method," *Journal of Thermal Science and Engineering Applications*, vol. 9, no. 1, article 011003, 2017.

[15] O. Mahian, A. Kianifar, S. Z. Heris, D. Wen, A. Z. Sahin, and S. Wongwises, "Nanofluids effects on the evaporation rate in a solar still equipped with a heat exchanger," *Nano Energy*, vol. 36, pp. 134–155, 2017.

[16] X. Qiang, I. Siddique, K. Sadiq, and N. A. Shah, "Double diffusive MHD convective flows of a viscous fluid under influence of the inclined magnetic field, source/sink and chemical reaction," *Alexandria Engineering Journal*, vol. 59, no. 6, pp. 4171–4181, 2020.

[17] I. Siddique, K. Sadiq, I. Khan, and K. S. Nisar, "Nanomaterials in convection flow of nanofluid in upright channel with gradients," *Journal of Materials Research and Technology*, vol. 11, pp. 1411–1423, 2021.

[18] R. Gupta, M. Gaur, Q. Al-Mdallal, S. D. Purohit, and D. L. Suthar, "Numerical study of the flow of two radiative nanofluids with Marangoni convection embedded in porous medium," *Journal of Nanomaterials*, vol. 2022, 7 pages, 2022.

[19] T. Gohar, S. Khan, N. Sene, A. Mouldi, and A. Brahmia, "Heat and mass transfer of the Darcy-Forchheimer Casson hybrid nanofluid flow due to an extending curved surface," *Journal of Nanomaterials*, vol. 2022, 12 pages, 2022.

[20] W. Ashraf, A. H. Alghtani, I. Khan, and M. Andualem, "Andualem. Thermal transport in radiative nanofluids by considering the influence of convective heat condition," *Journal of Nanomaterials*, vol. 2022, Article ID 1854381, 11 pages, 2022.

[21] M. Zaka Ullah, D. Abuzaid, and M. Asma, "Abdul Bariq. Couple stress hybrid nanofluid flow through a converging-diverging channel," *Journal of Nanomaterials*, vol. 2021, Article ID 2355258, 13 pages, 2021.

[22] K. Sadiq, I. Siddique, R. Ali, and F. Jarad, "Impact of ramped concentration and temperature on MHD Casson nanofluid flow through a vertical channel," *Journal of Nanomaterials*, vol. 2021, Article ID 3743876, 17 pages, 2021.

[23] H. Stehfest, "Algorithm 368: numerical inversion of Laplace transforms [D5]," *Communications of the ACM*, vol. 13, no. 1, pp. 47–49, 1970.

[24] D. Y. Tzou, *Macro to Microscale Heat Transfer, the Lagging Behavior*, Taylor and Francis, Washington, 1997.

[25] A. Talbot, "The accurate numerical inversion of Laplace transforms," *IMA Journal of Applied Mathematics*, vol. 23, no. 1, pp. 97–120, 1979.

[26] G. Honig and U. Hirdes, "A method for the numerical inversion of Laplace transforms," *Journal of Computational and Applied Mathematics*, vol. 10, no. 1, pp. 113–132, 1984.

[27] B. Davies, "Integral transforms and their applications," *AMS*, vol. 25, 2005.

[28] M. Turkyilmazoglu, "Exact analytical solutions for heat and mass transfer of MHD slip flow in nanofluids," *Chemical Engineering Science*, vol. 84, pp. 182–187, 2012.

[29] M. Hatami and D. D. Ganji, "Natural convection of sodium alginate (SA) non-Newtonian nanofluid flow between two vertical flat plates by analytical and numerical methods," *Case studies in thermal engineering*, vol. 2, pp. 14–22, 2014.

[30] A. Hajizadeh, N. A. Shah, F. D. Zaman, and I. L. Animasaun, "Analysis of natural convection bionanofluid between two vertical parallel plates," *Bionanosciences*, vol. 9, no. 4, pp. 930–936, 2019.